On approximations for a birth-death-movement process with correlations

Rasa Giniūnaitė[a]

Supervisors: Ruth E. Baker[a], Matthew J. Simpson[b]

[a] *Centre for Mathematical Biology, Mathematical Institute, University of Oxford, Oxford, UK.*

[b] *School of Mathematical Sciences, Queensland University of Technology, Brisbane, Australia.*

October 6, 2017

Abstract

Migration, proliferation and death are crucial processes in biological systems across different scales. They are important at the cellular level, for example during embryonic development, as well as for macroscale processes, where they govern the population dynamics of groups of organisms. Spatial heterogeneity often arises in such systems due to crowding and exclusion, depending on the relative rates of proliferation, migration and death. A logistic mean-field description is frequently used as a phenomenological model of birth and death, but it completely ignores spatial correlations between individuals. In this work we derive corrected mean-field descriptions of an on-lattice birth-death-movement process by incorporating pairwise interactions using a closure approximation. We extend previous work on regular square lattices to a hexagonal lattice. In addition, we outline existing moment closure approximations and apply a maximum entropy closure technique to the problem. We compare results with those obtained using the Kirkwood superposition approximation, which is the most frequently used for such systems, and observe that there is a significant improvement in the one-dimensional case but not in two-dimensions, thereby highlighting the sensitivity of closure approximations in general.

1 Introduction

Cell motility, proliferation and death are the key factors in the homeostasis, development and repair of organisms [1]. For example, understanding how cells migrate and proliferate is important for the inhibition of cancer metastasis, which is the major cause of death in cancer patients. Mathematical models could help us to identify the key factors that influence motility and growth, and therefore should be controlled. Hecht and co-workers modelled the cell movement and proliferation of tumour cells and showed that the co-existence of different cell clones in a tumour optimises its invasive ability [2]. Another example is the work on cell migration and proliferation during monolayer formation and wound healing by Tremel and co-workers [3]. They fitted

their model to the data and determined diffusion and growth parameters, which afterwards were used to explore behaviour of the cells on other surfaces and under different conditions. These examples show that modelling cell dynamics can produce insightful predictions for different biological systems.

Motility and proliferation are highly affected by the surroundings of the cell, including cell-to-cell interactions. For example, strong cell-to-cell adhesion or sufficiently rapid cell proliferation can lead to the clustering of an initially uniform population [4, 5]. A more specific example is the work by Jiao et al., in which statistical descriptors were used to characterise spatial distributions of benign brain white matter cells and brain glioma and quantify how pairs of cell nuclei are correlated in space in various ways [6]. They observed that cancer cells pack more densely than normal cells and exhibit stronger effective repulsions between any pair of cells. These examples demonstrate that the effects of spatial correlations play a crucial role in living systems, and therefore should be incorporated in mathematical models to provide accurate predictions.

Discrete individual-based models (IBMs) naturally incorporate spatial correlations [7–9], however they are computationally expensive and therefore not suitable for detailed investigations or, for example, parameter inference using approximate Bayesian computation, which requires numerous simulations of data sets from the model [10]. The logistic model is a mean-field approximation (MFA) of a simple birth-death-movement IBM [11, 12], which even has an analytic solution, however it neglects spatial correlations and is often therefore inaccurate at predicting the evolution of species density. A continuum description of an IBM that includes spatial correlations using pairwise approximations is a promising approach [13–23]. One of the difficulties in correcting the MFA, even for an IBM of birth-death-movement on a two-dimensional (2D) square lattice, is the numerical expense of encoding correlations at various lattice distances [15]. A common feature of the continuum description of systems with spatial correlations is the use of a closure approximation to truncate the set of ordinary differential equations (ODEs), which describe the dynamics of the occupancy of k-tuplets of lattice sites [15, 24, 25]. The Kirkwood superposition approximation (KSA) [20, 22] is the most widely applied for this problem [15, 18, 19, 26]. This choice is reasoned by comparing the performance of this closure with some other heuristic closures and the fact that it maximises the entropy, i.e. the choice of the approximation is the least biased [23, 27, 28]. However, it is important to note that the maximum entropy closure coincides with the KSA for systems on infinite domains but differs in finite systems, thus the rationale for its use is not entirely correct. The application of maximum entropy moment closure approximations were discussed for continuous space models in physics [27], ecology [23] and discrete time stochastic process in epidemiology [23]. Even though this moment closure framework seems to be promising, the results in favour of this approach were not robust, leaving the question of the most reliable closure technique open.

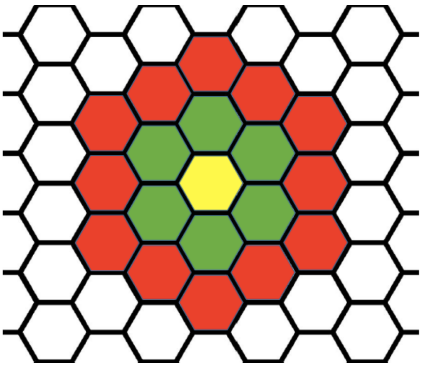

Figure 1: Hexagonal lattice, distances approximated as radial.

We address the issue of complexity of incorporation of pairwise correlations at various distances on a square lattice by replacing the lattice with a hexagonal one. Even though, at the first glance, it might seem that the implementation for a hexagonal lattice could be more complicated, it can in fact be simplified due to the similarity of the hexagonal lattice structure to concentric circles (Figure 1). Discrete simulations of an individual-based birth-death-movement model on a hexagonal lattice produce similar results to those of the same model implemented on a square lattice, with a slight increase observed in the final population numbers due to an increased number of neighbours, thus more flexibility for proliferation. We observe that a continuum approximation of the IBM that includes pairwise correlations produces a much better approximation of the IBM using the hexagonal lattice in comparison to the square lattice. In addition, we suggest a novel approach to incorporate boundary conditions in the truncated system, which correspond to approximation of the pairwise densities of distance greater than a certain threshold. Our results are remarkably improved using this approximation on the hexagonal lattice. Finally, we focus on the choice of closure technique and incorporate a maximum entropy closure for the triplets of sites that are all neighbours to each other, where the KSA closure is shown to produce the largest error. We demonstrate that in the one-dimensional (1D) case the improvement is remarkable, however in the 2D case on a hexagonal lattice there is no improvement. It is possible that due to the increased number of neighbours on the hexagonal lattice the KSA closure effectively maximises the entropy, as for the infinite system.

1.1 Aims for this work and outline

The aim of this work is to improve a coarse-grained description of the growth of a population of cells undergoing a birth-death-movement process with volume exclusion and with inclusion of the occupancy correlations between pairs of lattice sites. We do so by replacing the square lattice with a hexagonal one. In addition, we suggest optimal boundary conditions for a truncated system of ODEs describing the dynamics of the density and pairwise density at different distances. We apply the KSA closure to approximate the dynamics of triplets at all the distances except those where the triplets are neighbours. In this case we apply a maximum entropy closure technique. The remainder of this report is organised as follows. In Section 2 we introduce the derivation of the model. In Section 3 we outline different closure techniques and apply the most promising ones

to the problem. We discuss the numerical methods used to solve the system of ODEs and generate discrete results in Section 4. We produce comparisons of different boundary conditions, lattices and types of moment closure in Section 5. The report concludes in Section 6 with a discussion of our results and suggestions for further research.

2 Model

2.1 Outline of the problem

We model an exclusion process on a ring lattice, square lattice in 2D and hexagonal lattice in 2D. Each lattice site may be occupied by at most one cell (A) and at any time the cell has a transition rate P_m per unit time of moving to a neighbouring lattice site, proliferation rate P_p per unit time of giving rise to another cell (in a neighbouring site), and a death rate P_d per unit time. Each of the processes of movement and proliferation may only take place if the target site is unoccupied (0). The spacing between lattice sites is fixed at δx, so that for example in 2D lattice sites can be identified by their index $i \in [1, L]$, $j \in [1, L]$ where L is the length of the domain. Periodic boundary conditions and uniform random initial conditions are imposed. We denote the number of cells on the lattice at time t by $Q(t)$.

2.2 Derivation of the coarse-grained model

We consider simple dynamics of cells, namely cells can move, proliferate or die, as described in Section 2.1, and the corresponding "reaction" equations are

$$A + 0 \xrightarrow{P_m} 0 + A, \tag{1}$$

$$A + 0 \xrightarrow{P_p} A + A, \tag{2}$$

$$A \xrightarrow{P_d} 0. \tag{3}$$

The aim is to accurately describe the changes in the total number of cells over time. We use k-point density functions $\rho^{(k)}$ $(k = 1, 2, ...)$ [15, 24, 25], which describe the occupancy of k-tuplets of lattice sites, to keep track of the quantity of interest. This allows us to incorporate correlations between different cells which is neglected in the logistic growth approximation.

We define $\boldsymbol{l}$ and $\boldsymbol{m}$ to be vectors that point to sites on the lattice, $\sigma_l \in \{0, A\}$ to be the lattice variable which describes the state of lattice site $\boldsymbol{l}$, where A corresponds to an occupied site and 0 to an empty site. Let $z = 2d$ be the lattice constant for the square lattice (d - dimension of the lattice), this is the number of nearest neigbours (for the hexagonal lattice $z = 6$).

For $k = 1$ the density function corresponds simply to the probability of the site $\boldsymbol{l}$ being occupied by a cell and, since we chose uniform random initial conditions, does not depend on $\boldsymbol{l}$. We may write

$$\rho^{(1)}(A_l) = c, \qquad \rho^{(1)}(0_l) = c_0 = 1 - c, \tag{4}$$

where c is the fractional density of cells.

For $k = 2$ the density function depends only on $|\boldsymbol{l} - \boldsymbol{m}|$ due to the translational invariance of the lattice, i.e. with a slight abuse of notation we can write

$$\rho^{(2)}(A_l, A_m) = \rho^{(2)}(|\boldsymbol{l} - \boldsymbol{m}|). \tag{5}$$

Note that for the terms of the form $\rho^{(2)}(A_l, 0_m)$, we can use the conservation law $\rho^{(2)}(0_l, A_m) + \rho^{(2)}(A_l, A_m) = \rho^{(1)}(A_m) = c$. In the description of the evolution of the two-point density functions, we require three-point density functions, $\rho^{(3)}$, which satisfy a similar conservation rule

$$\sum_{\sigma_n} \rho^{(3)}(\sigma_l, \sigma_m, \sigma_n) = \sigma^{(2)}(\sigma_l, \sigma_m). \tag{6}$$

We also define $\alpha_{n,l}$ as an indicator function of nearest neighbour lattice sites:

$$\alpha_{n,l} = \begin{cases} 1, \text{ if } \boldsymbol{n} \text{ and } \boldsymbol{l} \text{ are nearest neighbours,} \\ 0, \text{ otherwise.} \end{cases} \tag{7}$$

2.3 One-point density functions

The rate of change of one-point density functions is affected by movement from nearest neighbour sites, proliferation from neighbouring sites and the death of the agent on the site. This can be expressed as

$$\frac{\mathrm{d}\rho^{(1)}(A_l)}{\mathrm{d}t} = P_m \sum_n \frac{\alpha_{n,l}}{z} \left[\rho^{(2)}(0_l, A_n) - \rho^{(2)}(A_l, 0_n)\right] + P_p \sum_n \frac{\alpha_{n,l}}{z} \rho^{(2)}(0_l, A_n) - P_d \rho^{(1)}(A_l). \tag{8}$$

We use the conservation laws

$$\rho^{(2)}(0_l, A_n) + \rho^{(2)}(A_l, A_n) = \rho^{(1)}(A_n) = c, \tag{9}$$

$$\rho^{(2)}(A_l, 0_n) + \rho^{(2)}(A_l, A_n) = \rho^{(1)}(A_l) = c, \tag{10}$$

to eliminate the motility terms, and knowledge about the nearest neighbours to obtain a simplification of equation (8)

$$\frac{\mathrm{d}c}{\mathrm{d}t} = P_p \left(c - \rho^{(2)}(1)\right) - P_d c. \tag{11}$$

It is important to note that if we assume that the neighouring sites are independent, i.e. $\rho^{(2)}(1) = c^2$, then equation (11) reduces to the logistic equation [29]. For simplification in this case, we rescale the system using

$$\bar{c} = \frac{P_p}{P_p - P_d} c \to \frac{\mathrm{d}\bar{c}}{\mathrm{d}t} = r\bar{c}(1 - \bar{c}), \tag{12}$$

with solution

$$\bar{c}(t) = \frac{\bar{c}(0)e^{rt}}{1 + \bar{c}(0)(e^{rt} - 1)}, \tag{13}$$

where $r = (P_p - P_d)$ and $\bar{c}(0) = ((P_p - P_d)/P_p)c(0)$. For further simplification, and provided that $r = (P_p - P_d) > 0$ to avoid negative time, we can rescale time $\bar{t} = (P_p - P_d)t$ to obtain

$$\bar{c}(\bar{t}) = \frac{\bar{c}(0)e^{\bar{t}}}{1 + \bar{c}(0)(e^{\bar{t}} - 1)}. \tag{14}$$

The mean-field logistic approximation obtained by simplifying equation (11) to equation (14) ignores spatial correlations, which in many cases might not be a valid assumption. We will use the analytical solution of the logistic equation to compare with our models which incorporate spatial correlations.

2.4 Two-point density functions

For the general case we have

$$\begin{aligned}\frac{\mathrm{d}\rho^{(2)}(A_l,A_m)}{\mathrm{d}t} =& P_m\sum_{n\neq l}\frac{\alpha_{n,m}}{z}\left[\rho^{(3)}(A_l,0_m,A_n)-\rho^{(3)}(A_l,A_m,0_n)\right]\\ &+P_m\sum_{n\neq m}\frac{\alpha_{n,l}}{z}\left[\rho^{(3)}(0_l,A_m,A_n)-\rho^{(3)}(A_l,A_m,0_n)\right]-2P_d\rho^{(2)}(A_l,A_m)\\ &+P_p\left[\sum_{n\neq l}\frac{\alpha_{n,m}}{z}\rho^{(3)}(A_l,0_m,A_n)+\sum_{n\neq m}\frac{\alpha_{n,l}}{z}\rho^{(3)}(0_l,A_m,A_n)\right]\\ &+P_p\frac{\alpha_{l,m}}{z}\left[\rho^{(2)}(A_l,0_m)+\rho^{(2)}(0_l,A_m)\right], \end{aligned} \tag{15}$$

which can be simplified using the conservation rules to

$$\begin{aligned}\frac{\mathrm{d}\rho^{(2)}(A_l,A_m)}{\mathrm{d}t} =& 2P_m\sum_{n\neq l}\frac{\alpha_{n,m}}{z}\left[\rho^{(2)}(A_l,A_n)-\rho^{(2)}(A_l,A_m)\right]-2P_d\rho^{(2)}(A_l,A_m)\\ &+P_p\frac{\alpha_{l,m}}{z}\left[\rho^{(2)}(A_l,0_m)+\rho^{(2)}(0_l,A_m)\right]+2P_p\sum_{n\neq l}\frac{\alpha_{n,m}}{z}\rho^{(3)}(A_l,0_m,A_n). \end{aligned} \tag{16}$$

The triplet density function in the term involving proliferation means that the system of ODEs describing the two-point density functions is not closed. To close the system we need to approximate the triplet density functions in terms of pairwise and single density functions. In the next section we will consider different approaches to choose this approximation.

3 Closure approximations

Closure problems are pervasive in population models. It is common to consider only the average density (one-point density functions) and spatial covariance terms (two-point density functions) and approximate the triplet density functions. Within the literature, closure approximations have been derived using a range of approaches, based on methods for moments with varying degree of complexity and success, among which we have:

- *heuristic reasoning*, where closing relationships are constructed in a heuristic fashion, to satisfy various conditions for valid moment closure [21, 22, 30];
- *distributional properties*, where closures are derived assuming that we know the statistical distribution of the process [31–36];
- *variational methods*, where unknown distribution optimises some meaningful functional [23, 27, 28, 37].

In this report we will discuss closures based on heuristic reasoning since they have so far been the dominant ones in the field. We will select the most accurate closure for our model and compare it with the maximum entropy closure approach, which is a variational method.

3.1 Heuristic approximations

The choice of the moment closure is restricted by some qualitative features that a valid moment closure should possess [21, 22]. For the triplet approximation the key qualities involve positivity of the approximation and invariance under interchanging triplet members. These qualities are based on the definition of the third moment but there are other important conditions that arise from averaging and large-distance limits, and qualities from dynamical invariance under relabelling. We consider three most commonly applied closures of different powers. The power is determined by the number of pair densities that are multiplied by each other. These closures satisfy different conditions and therefore differ in performance under different circumstances [22].

- The **power 1** closure we employ can be derived by setting the third central moments equal to those of Gaussian [33], i.e. setting them to zero. This gives

$$\begin{aligned}\rho^{(3)}(A_l, O_m, A_n) =&\rho^{(2)}(A_l, A_n)\rho^{(1)}(0_m) + \rho^{(1)}(A_n)\rho^{(2)}(A_l, O_m) \\ &+ \rho^{(1)}(A_l)\rho^{(2)}(0_k, A_n) - 2\rho^{(1)}(A_l)\rho^{(1)}(0_m)\rho^{(1)}(A_n). \end{aligned} \tag{17}$$

- The symmetric **power 2** we employ closure was originally suggested by Dieckmann and MacDonald [21] in analogy to the classical pair approximation and is of the form

$$\begin{aligned}\rho^{(3)}(A_l, 0_m, A_n) =&\frac{1}{2}\Bigg(\frac{\rho^{(2)}(A_l, 0_m)\rho^{(2)}(A_l, A_n)}{\rho^{(1)}(A_l)} + \frac{\rho^{(2)}(A_l, 0_m)\rho^{(2)}(0_m, A_n)}{\rho^{(1)}(0_m)} \\ &+ \frac{\rho^{(2)}(A_l, A_n)\rho^{(2)}(0_m, A_n)}{\rho^{(1)}(A_n)} - \rho^{(1)}(A_m)\rho^{(1)}(0_m)\rho^{(1)}(A_n)\Bigg). \end{aligned} \tag{18}$$

- The **power 3** closure we employ, also called the Kirkwood superposition approximation (KSA), has its origins in theoretical physics [38]. The key assumption under this closure is that at least two of the sites are sufficiently far apart and independent, in which case Bayes' Theorem gives

$$\rho^{(3)}(0_l, A_m, A_n) = \frac{\rho^{(2)}(0_l, A_n)\rho^{(2)}(0_l, A_m)\rho^{(2)}(A_m, A_n)}{\rho^{(1)}(0_l)\rho^{(1)}(A_m)\rho^{(1)}(A_n)}. \tag{19}$$

These approximations could be altered by weighting the various terms in the power 1 and the power 2 closures [22]. In addition, a combination of the closure techniques could be used [30]. However, such techniques are usually problem- and parameter-dependent. A comparison of these techniques for our problem conveyed that the KSA approximation significantly outperforms the other closures, therefore we will use it for further comparisons with the non-heuristic maximum entropy closure.

We use the KSA to close equation (16). Note that due to the translational invariance of the lattice, the density function $\rho^{(2)}(\sigma_l, \sigma_m)$ only depends on $|\boldsymbol{l} - \boldsymbol{m}|$. This together with the conservation rule gives the closed system equations

$$\frac{\mathrm{d}c}{\mathrm{d}t} = P_p\left(c - \rho^{(2)}(1)\right) - P_d c, \tag{20}$$

$$\frac{\mathrm{d}\rho^{(2)}(|\boldsymbol{l}-\boldsymbol{m}|)}{\mathrm{d}t} = 2P_m \sum_{n\neq l} \frac{\alpha_{n,m}}{z}\left[\rho^{(2)}(|\boldsymbol{l}-\boldsymbol{n}|) - \rho^{(2)}(|\boldsymbol{l}-\boldsymbol{m}|)\right] - 2P_d\rho^{(2)}(|\boldsymbol{l}-\boldsymbol{m}|)$$
$$+ 2P_p\frac{\alpha_{l,m}}{z}\left[c-\rho^{(2)}(|\boldsymbol{l}-\boldsymbol{m}|)\right] + 2P_p\sum_{n\neq l}\frac{\alpha_{n,m}}{z}\frac{(c-\rho^{(2)}(|\boldsymbol{l}-\boldsymbol{m}|))(c-\rho^{(2)}(|\boldsymbol{m}-\boldsymbol{n}|))\rho^{(2)}(|\boldsymbol{l}-\boldsymbol{n}|)}{c^2(1-c)}, \tag{21}$$

and we define $\rho^{(2)}(|\boldsymbol{l}-\boldsymbol{m}|)=0$ if $c=0$ and $\rho^{(2)}(|\boldsymbol{l}-\boldsymbol{m}|)=1$ if $c=1$ $\forall \boldsymbol{l},\boldsymbol{m}$.

3.2 Maximum entropy closure

In statistical mechanics the KSA is a good approximation of the triplet density functions in terms of pairwise and single density functions when at least two particles are sufficiently far apart and independent [38,39]. Therefore, it is important to seek a different type of closure for proximal lattice sites. We consider a maximum entropy closure approach as a potential replacement for the KSA for lattice sites a small distance apart.

We consider the definition of entropy based on the information theoretic point of view. This means that entropy describes the uncertainty of the outcome of a random variable. The fathers of information theory Shannon, Weaver and Khinchin [40,41] showed that the information content of a particular outcome $(x'+\mathrm{d}x')$ of random variable x with probability density $p(x)$, is given by $\ln[p(x')\mathrm{d}x']$. They also defined an entropy functional as the expectation of the information content over all possible outcomes x. For example, if we have a uniform distribution on an interval, the uncertainty about a specific outcome of the random variable is maximal, hence if there are no additional constraints the entropy functional is maximised for this distribution. The opposite case is when there is no uncertainty and the entropy is null, in our example this would correspond to the Dirac delta distribution.

Maximisation of entropy can be used to estimate unknown probability distributions of any system based on the average properties of that system, because we would obtain distributions that have the least bias with respect to the known information [40–42]. This approach has been used to develop moment-closure approximations for space models [23, 27, 28]. We use the ideas developed by Singer [27] to derive a maximum entropy closure for our model because it is the most suitable for our problem.

We will consider specific sites on the lattice explicitly for the sake of clarity, and then generalise to distances. An approximate closure relation can be found by maximishing the triplet entropy functional:

$$H\left(\rho^{(3)}(\sigma_l,\sigma_m,\sigma_n)\right) = -\sum_{X=A,0}\rho^{(3)}(X_l,X_m,X_n)\times\ln\,\rho^{(3)}(X_l,X_m,X_n), \tag{22}$$

under the constraints arising from the conservation law equations (23):

$$\begin{aligned}
\phi_1\left(\rho^{(3)}(\sigma_l,\sigma_m,\sigma_n)\right) &= \sum_{X=A,0}\rho^{(3)}(\sigma_l,\sigma_m,X_n) - \rho^{(2)}(\sigma_l,\sigma_m) = 0;\\
\phi_2\left(\rho^{(3)}(\sigma_l,\sigma_m,\sigma_n)\right) &= \sum_{X=A,0}\rho^{(3)}(\sigma_l,X_m,\sigma_n) - \rho^{(2)}(\sigma_l,\sigma_n) = 0;\\
\phi_3\left(\rho^{(3)}(\sigma_l,\sigma_m,\sigma_n)\right) &= \sum_{X=A,0}\rho^{(3)}(X_l,\sigma_m,\sigma_n) - \rho^{(2)}(\sigma_m,\sigma_n) = 0.
\end{aligned} \tag{23}$$

This variational problem can be solved by the method of Lagrange multipliers. We define Lagrange multipliers $\lambda_1(\sigma_m, \sigma_n), \lambda_2(\sigma_l, \sigma_n), \lambda_3(\sigma_l, \sigma_m)$ and the functional

$$F\left(\rho^{(3)}, \lambda_1, \lambda_2, \lambda_3\right) = H\left(\rho^{(3)}\right) + \lambda_1\phi_1 + \lambda_2\phi_2 + \lambda_3\phi_3. \tag{24}$$

The Euler-Lagrange equation of this functional is:

$$-\ln \rho^{(3)}(\sigma_l, \sigma_m, \sigma_n) - 1 + \lambda_1(\sigma_m, \sigma_n) + \lambda_2(\sigma_l, \sigma_m) + \lambda_3(\sigma_l, \sigma_n) = 0, \tag{25}$$

which can be used to derive the expression for $\rho^{(3)}$:

$$\rho^{(3)}(\sigma_l, \sigma_m, \sigma_n) = \gamma_1(\sigma_m, \sigma_n)\gamma_2(\sigma_l, \sigma_n)\gamma_3(\sigma_l, \sigma_m), \tag{26}$$

where

$$\gamma_1 = e^{\lambda_1(\sigma_m, \sigma_n) - \frac{1}{3}},$$

$$\gamma_2 = e^{\lambda_2(\sigma_l, \sigma_n) - \frac{1}{3}},$$

$$\gamma_3 = e^{\lambda_3(\sigma_l, \sigma_m) - \frac{1}{3}}.$$

Note that since the constraints equations (23) are all of the same form, the Lagrange multipliers can be interchanged, and thus we can set $\gamma_1 = \gamma_2 = \gamma_3 = \gamma$. Hence

$$\rho^{(3)}(\sigma_l, \sigma_m, \sigma_n) = \gamma(\sigma_m, \sigma_n)\gamma(\sigma_l, \sigma_n)\gamma(\sigma_l, \sigma_m). \tag{27}$$

The constraint that $\rho^{(2)}$ is the marginal of $\rho^{(3)}$ gives an equation for γ:

$$\rho^{(2)}(\sigma_l, \sigma_m) = \gamma(\sigma_l, \sigma_m) \sum_{X=A,0} \gamma(\sigma_l, X_n)\gamma(\sigma_m, X_n). \tag{28}$$

Recall that the open system of one-point and two-point density functions that we want to solve consists of equations

$$\frac{\mathrm{d}c}{\mathrm{d}t} = P_p\left(c - \rho^{(2)}(1)\right) - P_d c, \tag{29}$$

$$\begin{aligned}\frac{\mathrm{d}\rho^{(2)}(A_l, A_m)}{\mathrm{d}t} =& 2P_m \sum_{n\neq l} \frac{\alpha_{n,m}}{z}\left[\rho^{(2)}(A_l, A_n) - \rho^{(2)}(A_l, A_m)\right] - 2P_d^{(2)}(A_l, A_m) \\ &+ P_p\frac{\alpha_{l,m}}{z}\left[\rho^{(2)}(A_l, 0_m) + \rho^{(2)}(0_l, A_m)\right] + 2P_p \sum_{n\neq l} \frac{\alpha_{n,m}}{z}\rho^{(3)}(A_l, 0_m, A_n).\end{aligned} \tag{30}$$

We can close the system of equations (29)-(30) by substituting the triplet approximation (27) into equation (30):

$$\begin{aligned}\frac{\mathrm{d}\rho^{(2)}(A_l, A_m)}{\mathrm{d}t} =& 2P_m \sum_{n\neq l} \frac{\alpha_{n,m}}{z}\left[\rho^{(2)}(A_l, A_n) - \rho^{(2)}(A_l, A_m)\right] - 2P_d^{(2)}(A_l, A_m) \\ &+ P_p\frac{\alpha_{l,m}}{z}\left[\rho^{(2)}(A_l, 0_m) + \rho^{(2)}(0_l, A_m)\right] + 2P_p \sum_{n\neq l} \frac{\alpha_{n,m}}{z}\gamma(0_m, A_n)\gamma(A_l, A_n)\gamma(A_l, 0_m).\end{aligned} \tag{31}$$

At this point we can again use the translational invariance to replace the references to specific sites A_l, A_m by considering the two-point densities of sites $|\boldsymbol{l} - \boldsymbol{m}|$ apart:

$$\frac{\mathrm{d}c}{\mathrm{d}t} = P_p\left(c - \rho^{(2)}(1)\right) - P_d c, \tag{32}$$

$$\frac{\mathrm{d}\rho^{(2)}(|\boldsymbol{l}-\boldsymbol{m}|)}{\mathrm{d}t} = 2P_m \sum_{n\neq l} \frac{\alpha_{n,m}}{z}\left[\rho^{(2)}(|\boldsymbol{l}-\boldsymbol{n}|) - \rho^{(2)}(|\boldsymbol{l}-\boldsymbol{m}|)\right] - 2P_d\rho^{(2)}(|\boldsymbol{l}-\boldsymbol{m}|)$$
$$+ 2P_p\frac{\alpha_{l,m}}{z}\left[c - \rho^{(2)}(|\boldsymbol{l}-\boldsymbol{m}|)\right] + 2P_p \sum_{n\neq l}\frac{\alpha_{n,m}}{z}\gamma_{A0}(|\boldsymbol{m}-\boldsymbol{n}|)\gamma_{AA}(|\boldsymbol{l}-\boldsymbol{n}|)\gamma_{A0}(|\boldsymbol{l}-\boldsymbol{m}|), \quad (33)$$

where $\gamma_{A0}(|\boldsymbol{m}-\boldsymbol{n}|) = \gamma(A_m, 0_n)$, $\gamma_{AA}(|\boldsymbol{l}-\boldsymbol{n}|) = \gamma(A_l, A_n)$. We will see that to compute $\gamma_{A0}(|\boldsymbol{m}-\boldsymbol{n}|)$ it is also necessary to find $\gamma_{00}(|\boldsymbol{m}-\boldsymbol{n}|) = \gamma(0_m, 0_n)$.

4 Numerical methods

In this section we discuss the numerical methods used to solve the system of coupled ODEs (20)-(21) and to generate discrete results. We used a ring of $L = 2000$ in 1D and $L \times L = 200 \times 200$ regular square lattice and the same size hexagonal lattice. We used periodic boundary conditions, random initial conditions, and average over 40 identically prepared realisations of our discrete system to compare to our closure approximation. Without loss of generality, we fix $P_m = 1.0$ throughout, and vary both P_p and P_d. It is not biologically realistic that the proliferation and death rates would be greater than the motility rate, therefore we assume that P_p and P_d cannot exceed P_m. We present results where initially each site is randomly occupied with probability 1/20 and 1/2. We plot results using rescaled time and density $\bar{t} = (P_p - P_d)t$, $\bar{c}_A = ((P_p - P_d)/P_p)c$ when $P_p \gg P_d$ and unscaled density and time for $P_p \geq\approx P_d$ and $P_p < P_d$ to observe the decrease in the population and avoid negative scaling, respectively.

4.1 Closure approximation

We solve the system of coupled ODEs numerically in MATLAB using a standard Runge-Kutta method with a constant time step of $\delta t = 0.01$. Since we use periodic boundary conditions, we do not need to solve the ODEs (20)-(21) for all distances up to length L but only for the distances up to $\tilde{L} = \lfloor L/2 \rfloor$. For a square lattice, based on the results from [15], we evaluate each distance between the sites up to the threshold $|\boldsymbol{l}-\boldsymbol{m}| = 5$ individually and move to a regular grid using a 2D Laplacian with radial/spherical symmetry to approximate the lattice Laplacian terms of equation (21) for $|\boldsymbol{l}-\boldsymbol{m}| > 5$. The Laplacian with radial symmetry that we use is of the form

$$\nabla^2 f(r) = \frac{\partial^2 f}{\partial r^2} + \frac{1}{r}\frac{\partial f}{\partial r} \approx \frac{f(r_{i-1}) - 2f(r_i) + f(r_{i+1})}{(\delta r)^2} + \frac{1}{r_i}\frac{f(r_{i+1}) - f(r_{i-1})}{\delta r}. \quad (34)$$

The main difference between a 2D hexagonal lattice and a square lattice is the number of neighbours, a site on a hexagonal lattice has six neighbours, as in the three-dimensional case, whereas only four for a square lattice. This makes the hexagonal lattice more accurate representation of biological systems [43, 44]. We define the distance between two sites as the number of edges that one has to cross when going from one to the other. Therefore if we consider sites n distance apart, the distances between a fixed site and the six neighbours of the other one are $n-1$, $n-1$, n, n, $n+1$, $n+1$ (Figure 2). This makes the approximations of different

distances much simpler than on the square lattice in 2D where we considered each actual distance separately (i.e. $1, \sqrt{2}, 2, \sqrt{5}, ...$) and approximated greater distances than five using radial symmetry.

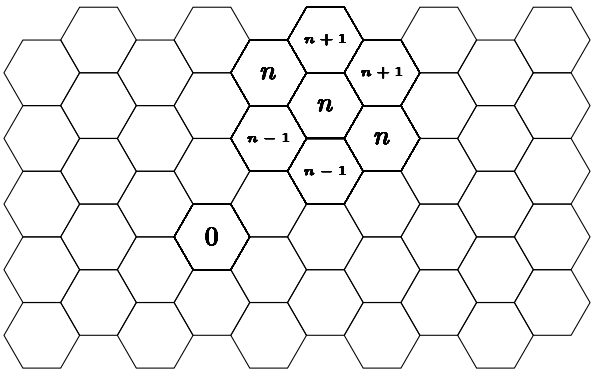

Figure 2: Hexagonal lattice with approximated distances.

Initial conditions. We choose a random initial seeding, each site is randomly occupied with probability 1/20 and 1/2, therefore initially all the sites are uncorrelated and $\rho^{(2)}(|\boldsymbol{l}-\boldsymbol{m}|) = c^2$, $\forall \boldsymbol{l}, \boldsymbol{m}$ at $t = 0$.

Boundary conditions. To start with we simply use periodic boundary conditions, but in fact we observe that we can truncate our system and then we assume that sites that are sufficiently far away are independent, therefore we set that $\rho^{(2)}(r_{max}) = c^2$ for the 1D and 2D square lattices. However, we explore another setting $\rho^{(2)}(r_{max}) = \rho^{(2)}(r_{max} - 1)$ which provides a better boundary approximation for a truncated system for the hexagonal lattice, we investigate this in greater detail in Section 5.1.

4.2 Maximum entropy

The following scheme, with a simplification in *Step 5* discussed after the algorithm, is used to find the triplet approximation and solve the system. To avoid notational confusion denote $\rho^{(2)} = \rho_2$. Recall $\tilde{L} = \lfloor L/2 \rfloor$, where L is the length of the domain or, if the system is truncated, $\tilde{L}$ is the length of the truncated system and set $|\boldsymbol{l}-\boldsymbol{m}| = r$.

Step 1 Provide initial guesses $\gamma^{(0)}_{AA}(r)$, $\gamma^{(0)}_{A0}(r)$ and $\gamma^{(0)}_{00}(r)$ for $1 \leq r \leq \tilde{L}$.

Step 2 Provide initial conditions based on the initial density of cells c at $t = 0$ and $\rho_2(r) = c^2$ at $t = 0$ for $1 \leq r \leq \tilde{L}$. Set $t = 0$.

Step 3 Set $i = 0$.

Step 4 Solve equations (35) - (36) with $|\boldsymbol{l}-\boldsymbol{m}|$ for c, ρ_2, over one time step $\mathrm{d}t$:

$$\frac{\mathrm{d}c}{\mathrm{d}t} = P_p\left(c - \rho_2(1)\right) - P_d c, \tag{35}$$

$$\frac{\mathrm{d}\rho_2(r)}{\mathrm{d}t} =2P_m \sum_{n\neq l} \frac{\alpha_{n,m}}{z} \left[\rho_2(|\boldsymbol{l}-\boldsymbol{n}|) - \rho_2(|\boldsymbol{l}-\boldsymbol{m}|)\right] - 2P_d\rho_2(|\boldsymbol{l}-\boldsymbol{m}|) + 2P_p\frac{\alpha_{l,m}}{z}\left[c-\rho_2(|\boldsymbol{l}-\boldsymbol{m}|)\right] + 2P_p\sum_{n\neq l}\frac{\alpha_{n,m}}{z}\rho^{(3)}(A_l,0_m,A_n), \tag{36}$$

where for $|\boldsymbol{l}-\boldsymbol{m}|=1$, $\rho^{(3)}(A_l,0_m,A_n)$ is approximated using the maximum entropy closure, i.e. $\rho^{(3)}(A_l,0_m,A_n) = \gamma^{(i)}_{A0}(|\boldsymbol{l}-\boldsymbol{m}|)\gamma^{(i)}_{AA}(|\boldsymbol{l}-\boldsymbol{n}|)\gamma^{(i)}_{A0}(|\boldsymbol{m}-\boldsymbol{n}|)$ and using the KSA otherwise.

Step 5 Solve the appropriate equations derived from equation (28) for $\gamma^{(i+1)}_{AA}$, $\gamma^{(i+1)}_{A0}$ and $\gamma^{(i+1)}_{00}$:

$$\begin{aligned}
\rho_2(r) &= \gamma^{(i+1)}_{AA}(r)\sum_{X=A,0}\gamma^{(i+1)}_{AX}(k)\left[\gamma^{(i+1)}_{AX}(|k-r|)+\gamma^{(i+1)}_{AX}(\min(r+k,|r+k-L|))\right],\\
c-\rho_2(r) &= \gamma^{(i+1)}_{A0}(r)\sum_{X=A,0}\gamma^{(i+1)}_{AX}(k)\left[\gamma^{(i+1)}_{0X}(|k-r|)+\gamma^{(i+1)}_{AX}(\min(r+k,|r+k-L|))\right],\\
1-2c+\rho_2(r) &= \gamma^{(i+1)}_{00}(r)\sum_{X=A,0}\gamma^{(i+1)}_{0X}(k)\left[\gamma^{(i+1)}_{0X}(|k-r|)+\gamma^{(i+1)}_{AX}(\min(r+k,|r+k-L|))\right],
\end{aligned} \tag{37}$$

for $\forall k \in [1,\tilde{L}]\setminus\{r\}$

Step 6 $i \leftarrow i+1$. Return to *Step 4*, until convergence of γ is achieved and set the value to which it converges to as $\gamma^{(final)}_{AA}$, $\gamma^{(final)}_{A0}$, $\gamma^{(final)}_{00}$.

Step 7 Set new initial conditions $c(t+\mathrm{d}t)=c(\mathrm{d}t)$ and $\rho_2(r)(t+\mathrm{d}t)=\rho_2(r)(\mathrm{d}t)$. Set $t=t+\mathrm{d}t$.

Step 8 If $t \geq t_{final}$ exit, otherwise set $\gamma^{(0)}_{AA}=\gamma^{(final)}_{AA}$, $\gamma^{(0)}_{A0}=\gamma^{(final)}_{A0}$ and $\gamma^{(0)}_{00}=\gamma^{(final)}_{00}$. Return to *Step 3* and continue solving the equations step by step.

Remarks:

- The left-hand side of equation (37) for the second and third equations is derived from $\rho_2(A,0)=\rho_1(A)-\rho_2(A,A)$ and $\rho_2(0,0)=\rho_1(0)-\rho_2(A,0)$.
- In *Step 5* we only consider constraints that involve neighbouring sites, i.e. $k=1$, which have the strongest correlations, thus reducing the computational costs.
- *Step 4* requires us to solve the system of ODEs step by step which is achieved using the Runge-Kutta method.
- The MATLAB in-built function *fsolve* is used to solve the constraints in equations (37) for $\gamma^{(i+1)}_{AA}$, $\gamma^{(i+1)}_{A0}$ and $\gamma^{(i+1)}_{00}$.
- Initially we set $\gamma^{(0)}_{AA}=1-c$ and $\gamma^{(0)}_{A0}=c$. However, this choice is not important; our investigation suggests that for different initial conditions γ_{AA}, γ_{A0} and γ_{00} converge to the same values.

4.3 Discrete simulations

The discrete model is simulated using a modified Gillespie approach [45] using the following algorithm:

Step 1 Set $t = 0$ and initialize the lattice by placing cells at the required lattice sites. Let $Q(t)$ be the number of cells.

Step 2 Calculate the total propensity function $a_0 = (P_m + P_p + P_d)Q(t)$. Let $\tau = (1/a_0)\log(1/r_1^u)$ where r_1^u is a uniform random number in the interval $[0, 1]$. If $t + \tau > t_{final}$ exit, otherwise go to *Step 3*.

Step 3 Decide whether a movement, proliferation or death occurs, according to the following: calculate $R = a_0 r_2^u$ where r_2^u is a uniform random number in the interval [0,1].

(i) If $R \in [0, P_m Q(t))$ execute a movement event. Choose an cell at random and a target site for movement from the nearest neighbors (of which there are two in 1D, four in 2D with a square lattice and six in 2D with a hexagonal lattice). If the target site is empty then move the cell into that site. If not, abort the movement event.

(ii) If $R \in [P_m Q(t), (P_m + P_p)Q(t))$ execute a proliferation event. Choose a cell at random and a target site for proliferation from the nearest neighbors (of which there are two in 1D, four in 2D with square lattice and six in 2D with hexagonal lattice). If the target site is empty then let the cell proliferate by placing a new cell in the target site and let $Q(t) \to Q(t) + 1$, $a_0 \to a_0 + (P_m + P_p + P_d)$. If not, abort the proliferation event.

(iii) If $R \in [(P_m + P_p)Q(t), (P_m + P_p + P_d)Q(t))$ execute a death event. Choose a cell at random and remove it from the system. Let $Q(t) \to Q(t) - 1$ and $a_0 \to a_0 - (P_m + P_p + P_d)$.

Step 4 Update time by letting $t \to t + \tau$ and return to Step 2.

5 Results

The aim of this work is improve the continuum approximations of IBMs which incorporate spatial effects. We achieve our aim by applying a novel approach to approximate boundary conditions, replacing a regular square lattice with a hexagonal one and introducing a maximum entropy closure technique. We present a representative subset of these results in this section.

5.1 Boundary conditions

We verified that the system of equations (20)-(21) can be truncated at $r_{max} = 3$ for both 2D square and hexagonal lattices without losing accuracy in the approximation, which is consistent with the results from [15] for the 2D square lattice. For this fixed $r_{max} = 3$, we use two different boundary conditions for the truncated system. First, one assumes that sites that are further than distance r_{max} apart are independent, i.e. $\rho^{(2)}(r) = c^2$

for $r > r_{max}$. Second, one assumes that the density of the sites further than distance r_{max} is the same as the density of the sites r_{max} apart, i.e. $\rho^{(2)}(r) = \rho^{(2)}(r_{max})$ for $r > r_{max}$. The results were not significantly different in these two cases for the square lattice but for the hexagonal lattice the second approach produced significantly better results (Figure 3). We only need to approximate the distance $r_{max} + 1$ on the hexagonal lattice because of our radial approximations and more different $r > r_{max}$ on the square lattice with actual distances. This might be a possible reason why the boundary condition $\rho^{(2)}(r) = \rho^{(2)}(r_{max})$ for $r > r_{max}$ performs less well on the square lattice.

It is worth mentioning that if the system is not truncated, i.e. $r_{max} > 3$, the latter boundary condition does not produce significantly better results than the former even for the hexagonal lattice. This is surprising because it means that for the second approach ($\rho^{(2)}(r) = \rho^{(2)}(r_{max})$ for $r > r_{max}$) the truncated system performs better than the full one. A possible explanation is that the error due to the distance approximation (in the hexagonal lattice we count the distance between two sites as the smallest number of edges that we need to cross to get from one site to the other) increases when r_{max} increases leading to a favourable result for small r_{max}.

In the following sections we will use the boundary condition $\rho^{(2)}(r) = c^2$ for $r > r_{max}$ for the square lattice and $\rho^{(2)}(r_{max} + 1) = \rho^{(2)}(r_{max})$ for the hexagonal lattice.

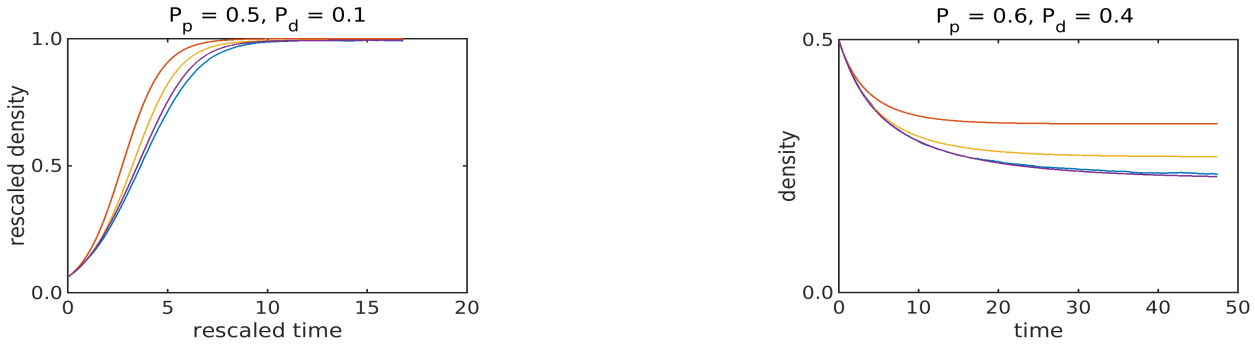

Figure 3: Comparison of different truncation approximations. Red - logistic, blue - Gillespie 2D on a hexagonal lattice averaged over 40 simulations, yellow - KSA with $\rho^{(2)}(r_{max}+1) = c^2$, purple - KSA with $\rho^{(2)}(r_{max}+1) = \rho^{(2)}(r_{max})$. The latter approach approximates the discrete simulations more accurately than the former one.

5.2 Comparison of different lattices

The main advantage of the hexagonal lattice in 2D is that each site has six neighbouring sites instead of four. An increased number of neighbouring sites over the square lattice allows more flexibility for cells to move around and proliferate in different directions and therefore the hexagonal lattice may represent reality more accurately. Figure 4 shows that there are always slightly more cells in the steady state when discrete simulations are performed on the hexagonal lattice (comparison of blue lines in the top row and bottom row). This difference is not significant, but what is worth pointing out is the improvement in the accuracy of the results given by the inclusion of correlations (yellow lines). The continuum approximation including spatial correlations on a hexagonal lattice (the bottom row, yellow line) matches with the Gillespie simulations (blue

line) much better than for the square lattice (the top row). This demonstrates that even though the distances are approximated as radial on the hexagonal lattice, making the implementation simpler than for the exact distances on the square lattice, more accurate approximations are obtained.

5.3 Comparison of different closure techniques

We now demonstrate the difference between the approximations when only the KSA closure is applied and when the closure for neighbouring triplets is obtained using entropy maximisation. Since based on a probabilistic interpretation, the KSA does not produce accurate approximations for triplets on neighbouring sites, one would expect that maximum entropy closure applied for this triplet should produce more accurate results, but in the following subsections we will see that this is only the case in 1D and surprisingly not in 2D.

5.3.1 1D case: KSA combined with maximum entropy versus KSA alone

Sites only have two neighbours in 1D, therefore the model including correlations and simple KSA closure, let alone mean-field logistic growth, produces poor approximations (Figure 5). Application of the maximum entropy closure leads to a significant improvement (purple line in Figure 5). This is an expected outcome since we avoid unreasonable KSA triplet approximations for neighbouring sites. However, it is important to note that the maximum entropy approximation is more computationally expensive (around 20 times slower) than just the KSA.

5.3.2 2D case on a hexagonal lattice: KSA combined with maximum entropy versus KSA alone

As we already observed in the bottom row of Figure 4, the KSA closure for the 2D hexagonal lattice produces reasonably accurate results. We would still expect the introduction of a maximum entropy closure to improve them, however we do not observe almost any change in the results when it is applied (Figure 6). This tendency could be explained by a decrease in the proportion of the triplets that are all neighbours to each other on a hexagonal lattice, and thus it becomes less significant to approximate them in a different way. Another possible explanation is the one suggested by Rogers [28], where he claims that an improved approximation scheme can even lead to worse results when used to close a system of differential equations due to the fortuitous cancellation of error in a simple approximation. Therefore, due to higher computational costs (around 20 times slower) for the application of maximum entropy approximation, we conclude that on a 2D hexagonal lattice for the closure of a system it is advisable to use the KSA alone.

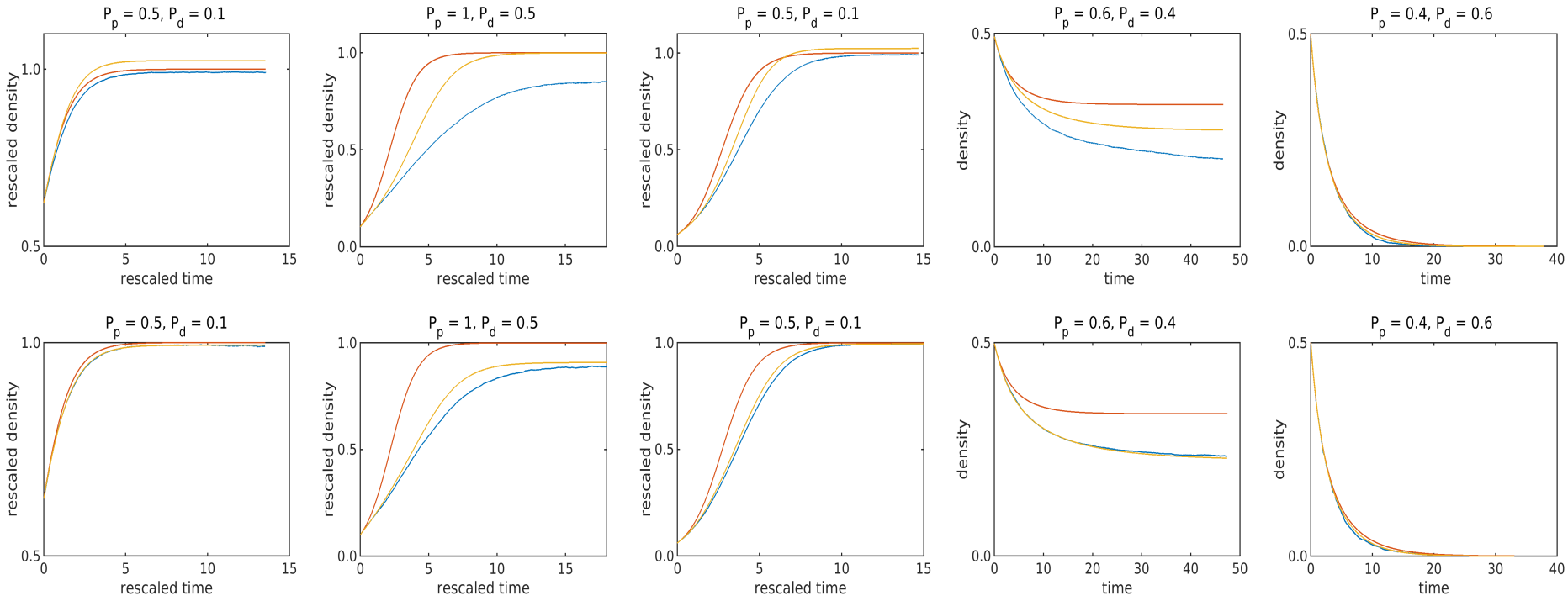

Figure 4: Comparison of simulations on different 2D lattices. Top row - KSA on a square lattice, bottom row - KSA on a hexagonal lattice. Red - logistic, blue - Gillespie 2D on a square (top row) and hexagonal (bottom row) lattices averaged over 40 simulations, yellow - KSA. The approximations on the hexagonal lattice outperform those on the square lattice under different parameter regimes.

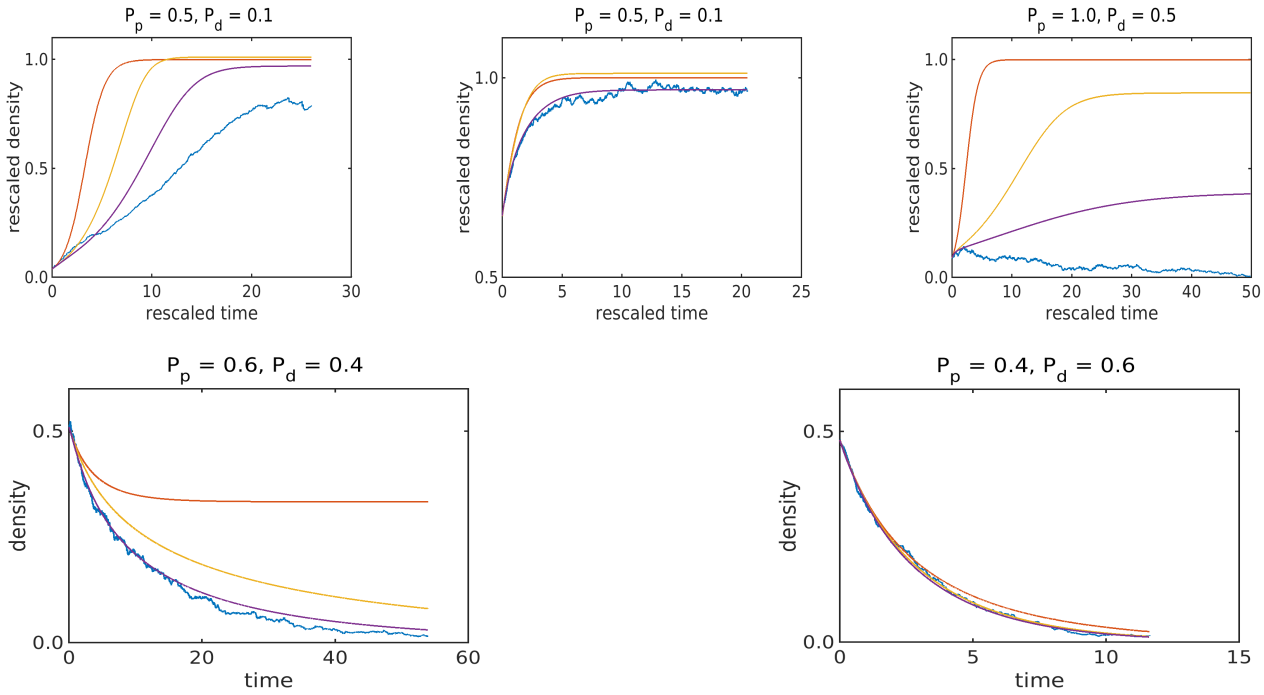

Figure 5: Simulations on a ring in the 1D case. Red - logistic, blue - Gillespie 1D averaged over 40 simulations, yellow - KSA, purple - maximum entropy combined with the KSA. The combination of the maximum entropy closure with the KSA outperforms the KSA alone.

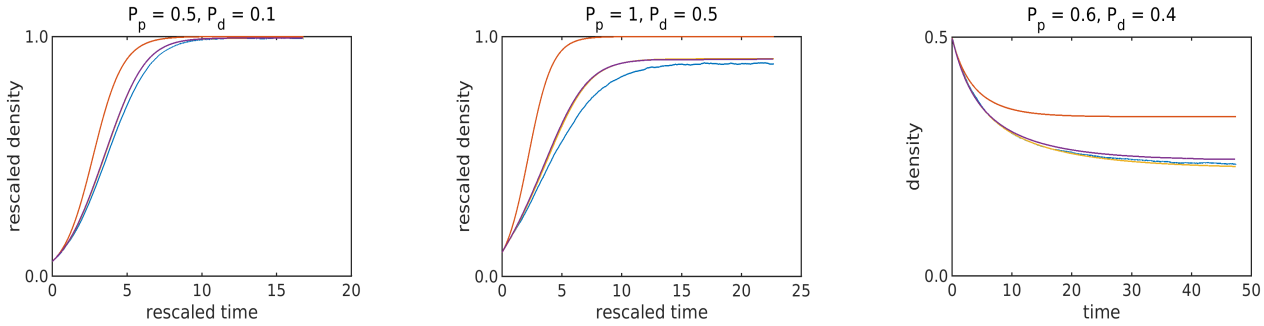

Figure 6: Simulations on a 2D hexagonal lattice. Red - logistic, blue - Gillespie 2D on a hexagonal lattice averaged over 40 simulations, yellow - KSA, purple - maximum entropy combined with the KSA. The incorporation of maximum entropy closure does not improve the approximations.

6 Discussion

The main focus of this work has been to improve continuum approximations of the an IBM when spatial correlations are significant. We started with a derivation of equations for the evolution of cell density including pairwise correlations between lattice sites and, to start with, used the KSA to close the system. We implemented the discrete Gillespie algorithm for a 1D ring and 2D square and hexagonal lattices. We compared averaged

discrete results with those of a standard logistic model and our continuum model that includes correlations. In agreement with the literature, the incorporation of correlations provided a vast improvement over the mean-field approximation. In addition, numerical results showed that the match between discrete simulations and our continuum correlation model is significantly better for the hexagonal lattice than for the square lattice. Due to the similarity of the hexagonal lattice structure to a radial mesh, we demonstrated that this approach resolves the inconvenience of the necessity to calculate the equations at each possible site separation on a square lattice. In both of the frameworks, the system of correlation equations could be truncated at a distance $r = 3$ without a loss in accuracy, and with a clear improvement in computational efficiency. We changed the assumption of the approximation of the pair density of the larger distance than threshold $r = 3$ from independent to equivalent to the pair density at the threshold distance and obtained remarkably better results. This alteration improves the accuracy of the prediction of the growth rates.

Throughout the first part of the work we used the KSA closure to truncate the system. This method seems to be most commonly used in the work on this problem [15, 18, 19, 26] and indeed provides a more accurate approximation than other most commonly used heuristic approaches (results not shown). However, variational methods have not been previously applied to the problem. The main drawback of the KSA is the inaccuracy of its approximation for neighbouring sites. To tackle this issue, we applied a maximum entropy closure for neighbouring triplets based on the ideas from [27]. We observed a vast improvement in the 1D case in comparison with the KSA closure alone. However, in a 2D case on a hexagonal lattice there was no significant improvement. It is important to note that the KSA in fact maximises the entropy for infinite systems [27], therefore we reasoned that an increase in the number of neighbouring sites might have contributed to the loss in the inaccuracy using the KSA closure alone. Another possible explanation is based on the arguments by Rogers [28], which he used to reason his observations that an improved maximum entropy approximation scheme leads to worse results than for the KSA. He claimed that a possible explanation of such a behaviour is a fortuitous cancellation of error and the lack of robustness and reliability in the predictions by moment-closure methods. This argument could also be used to explain our results, however this is still an open question and further investigation is needed.

The work could be improved by measuring actual discrepancies from the density of triplets of the discrete simulated results and the approximations of our continuum model with correlations. This would highlight the improvement on a hexagonal lattice and clarify the match of maximum entropy closure with the KSA for the 2D model on a hexagonal lattice. In addition, radially approximated distances on a hexagonal lattice could be replaced by actual distances. Even though this would be more complicated to incorporate, the improvement could be beneficial in case very accurate approximations are needed.

A significant improvement in approximations when boundary conditions were altered raises some interesting questions about the optimal boundary approximations. The mechanisms and reasons behind this improvement should be further investigated under different scenarios to reach a robust conclusion. These considerations are important because an improved boundary approximation could lead to a reduction in the size of systems without a great loss in accuracy, making the simulations less computationally expensive.

A possible extension of this work would be to validate its usefulness using biological data. The main benefit of this computationally less expensive modelling approach is for parameter inference. Approximate Bayesian computation (ABC) methods perform inference of model-specific parameters of mechanistically motivated parametric models when evaluating likelihoods is difficult [46]. This method involves the generation of a large number of sets from the parametric model of interest, therefore only applicable when the simulations are computationally inexpensive. One can easily see that our continuum model involving correlations could be used to infer parameters using ABC. Since we observed that our 2D hexagonal model approximates an IBM very accurately, we could obtain reliable estimations for birth, death and motility parameters. A specific example could be an investigation of growth-to-confluence assays for different cell lines.

References

[1] S. F. Gilbert. *Developmental Biology, 8th ed.* Sinauer Association Inc., Sunderland, MA, 2006.

[2] I. Hecht, S. Natan, A. Zaritsky, H. Levine, I. Tsarfaty, and E. Ben-Jacob. The motility-proliferation-metabolism interplay during metastatic invasion, vol. 5. p. 13538. 2015.

[3] A. Tremel, A. Cai, N. Tirtaatmadja, B. D. Hughes, G. Stevens, K. A. Landman, and A. J. O'Connor. Cell migration and proliferation during monolayer formation and wound healing, *Chemical Engineering Science.* vol. 64. no. 2. pp. 247–253. 2009.

[4] D. J. G. Agnew, J. E. F. Green, T. M. Brown, M. J. Simpson, and B. J. Binder. Distinguishing between mechanisms of cell aggregation using pair-correlation functions, *Journal of Theoretical Biology.* vol. 352. no. Supplement C. pp. 16 – 23. 2014.

[5] S. T. Johnston, M. J. Simpson, and R. E. Baker. Mean-field descriptions of collective migration with strong adhesion, *Phys. Rev. E.* vol. 85. p. 051922. 2012.

[6] Y. Jiao, H. Berman, T.-R. Kiehl, and S. Torquato. Spatial organization and correlations of cell nuclei in brain tumors, *PLOS ONE.* vol. 6. no. 11. pp. 1–9. 2011.

[7] G. B. Ermentrout and L. Edelstein-Keshet. Cellular automata approaches to biological modeling, *Journal of Theoretical Biology.* vol. 160. no. 1. pp. 97–133. 1993.

[8] P. Hogeweg. Cellular automata as a paradigm for ecological modeling, *Applied Mathematics and Computation.* vol. 27. no. 1. pp. 81–100. 1988.

[9] J. Moreira and A. Deutch. Cellular automaton models of tumor development: A critical review, *Advances in Complex Systems.* vol. 05. pp. 247–267. 2002.

[10] T. Toni, D. Welch, N. Strelkowa, A. Ipsen, and M. P. H. Stumpf. Approximate bayesian computation scheme for parameter inference and model selection in dynamical systems, *Journal of The Royal Society Interface.* vol. 6. no. 31. pp. 187–202. 2009.

[11] D. Hiebeler. Stochastic spatial models: From simulations to mean field and local structure approximations, *Journal of Theoretical Biology*. vol. 187. no. 3. pp. 307–319. 1997.

[12] M. A. M. de Aguiar, E. M. Rauch, and Y. Bar-Yam. Invasion and extinction in the mean field approximation for a spatial host-pathogen model, *Journal of Statistical Physics*. vol. 114. no. 5. pp. 1417–1451. 2004.

[13] K. J. Sharkey, C. Fernandez, K. L. Morgan, E. Peeler, M. Thrush, J. F. Turnbull, and R. G. Bowers. Pair-level approximations to the spatio-temporal dynamics of epidemics on asymmetric contact networks, *Journal of Mathematical Biology*. vol. 53. no. 1. pp. 61–85. 2006.

[14] K. J. Sharkey. Deterministic epidemic models on contact networks: Correlations and unbiological terms, *Theoretical Population Biology*. vol. 79. no. 4. pp. 115–129. 2011.

[15] R. E. Baker and M. J. Simpson. Correcting mean-field approximations for birth-death-movement processes, *Physical Review E*. vol. 82. p. 041905. 2010.

[16] U. Dieckmann and R. Law. *in The Geometry of Ecological Interactions: Simplifying Spatial Complexity*. Cambridge University Press, Cambridge, UK, pp. 412–455, 2000.

[17] N. Peyrard and A. Franc. Cluster variation approximations for a contact process living on a graph, *Physica A: Statistical Mechanics and its Applications*. vol. 358. no. 2. pp. 575–592. 2005.

[18] D. C. Markham, M. J. Simpson, and R. E. Baker. Simplified method for including spatial correlations in mean-field approximations, *Phys. Rev. E*. vol. 87. p. 062702. 2013.

[19] M. J. Simpson and R. E. Baker. Corrected mean-field models for spatially dependent advection-diffusion-reaction phenomena, *Phys. Rev. E*. vol. 83. p. 051922. 2011.

[20] R. Law, D. Murrell, and U. Dieckmann. Population growth in space and time: Spatial logistic equations, *Ecology*. vol. 84. no. 1. pp. 252–262. 2003.

[21] U. Dieckmann and G. J. MacDonald. Relaxation projections and the method of moments, *Interim Report IR-99-040*. 1999.

[22] D. J. Murrell, U. Dieckmann, and R. Law. On moment closures for population dynamics in continuous space, *Journal of Theoretical Biology*. vol. 229. no. 3. pp. 421–432. 2004.

[23] M. Raghib, N. A. Hill, and U. Dieckmann. A multiscale maximum entropy moment closure for locally regulated space–time point process models of population dynamics, *Journal of Mathematical Biology*. vol. 62. no. 5. pp. 605–653. 2011.

[24] J. Mai, V. N. Kuzovkov, and W. von Niessen. A theoretical stochastic model for the a+1/2b2→0 reaction, *The Journal of Chemical Physics*. vol. 98. no. 12. pp. 10017–10025. 1993.

[25] J. Mai, V. Kuzovkov, and W. von Niessen. A general stochastic model for the description of surface reaction systems, *Physica A: Statistical Mechanics and its Applications*. vol. 203. no. 2. pp. 298–315. 1994.

[26] D. C. Markham, M. J. Simpson, P. K. Maini, E. A. Gaffney, and R. E. Baker. Incorporating spatial correlations into multispecies mean-field models, *Phys. Rev. E.* vol. 88. p. 052713. 2013.

[27] A. Singer. Maximum entropy formulation of the kirkwood superposition approximation, *The Journal of Chemical Physics.* vol. 121. no. 8. pp. 3657–3666. 2004.

[28] T. Rogers. Maximum-entropy moment-closure for stochastic systems on networks, *Journal of Statistical Mechanics-Theory and Experiment.* vol. 2011. 2011.

[29] J. D. Murray. *Mathematical Biology I: An Introduction, 3rd e.* Berlin, Springer-Verlag, 2003.

[30] J. A. N. Filipe and M. M. Maule. Analytical methods for predicting the behaviour of population models with general spatial interactions, *Mathematical Biosciences.* vol. 183. no. 1. pp. 15–35. 2003.

[31] A. Singh and J. P. Hespanha. A derivative matching approach to moment closure for the stochastic logistic model, *Bulletin of Mathematical Biology.* vol. 69. no. 6. pp. 1909–1925. 2007.

[32] I. Z. Kiss and P. L. Simon. New moment closures based on a priori distributions with applications to epidemic dynamics, *Bulletin of Mathematical Biology.* vol. 74. no. 7. pp. 1501–1515. 2012.

[33] R. Grima. A study of the accuracy of moment-closure approximations for stochastic chemical kinetics, *The Journal of Chemical Physics.* vol. 136. no. 15. p. 154105. 2012.

[34] D. Schnoerr, G. Sanguinetti, and R. Grima. Comparison of moment-closure approximations for stochastic chemical kinetics, *The Journal of Chemical Physics.* vol. 143. 2015.

[35] E. Lakatos, A. Ale, P. D. W. Kirk, and M. P. H. Stumpf. Multivariate moment closure techniques for stochastic kinetic models, *The Journal of Chemical Physics.* vol. 143. no. 9. p. 094107. 2015.

[36] M. J. Keeling. Multiplicative moments and measures of persistence in ecology, *Journal of Theoretical Biology.* vol. 205. no. 2. pp. 269–281. 2000.

[37] T. Hillen. On the l2-moment closure of transport equations: the cattaneo approximation, discrete contin, *Dyn. Syst. Ser. B.* pp. 961–982. 2004.

[38] J. G. Kirkwood. Statistical mechanics of fluid mixtures, *The Journal of Chemical Physics.* vol. 3. no. 5. pp. 300–313. 1935.

[39] J. G. Kirkwood and E. M. Boggs. The radial distribution function in liquids, *The Journal of Chemical Physics.* vol. 10. no. 6. pp. 394–402. 1942.

[40] C. E. Shannon and W. Weaver. *The mathematical theory of communication.* University of Illinois Press, Champaign, 1949.

[41] A. I. Khinchin. *Mathematical foundations of information theory.* Dover, New York, 1957.

[42] E. T. Jaynes. Information theory and statistical mechanics, *Phys. Rev.*. vol. 106. pp. 620–630. 1957.

[43] G. A. Trunfio. *Predicting Wildfire Spreading Through a Hexagonal Cellular Automata Model.* pp. 385–394. Berlin, Heidelberg: Springer Berlin Heidelberg. 2004.

[44] S. Adachi, F. Peper, and J. Lee. *Universality of Hexagonal Asynchronous Totalistic Cellular Automata.* pp. 91–100. Berlin, Heidelberg: Springer Berlin Heidelberg. 2004.

[45] D. T. Gillespie. Exact stochastic simulation of coupled chemical reactions, *The Journal of Physical Chemistry.* vol. 81. no. 25. pp. 2340–2361. 1977.

[46] M. Sunnåker, A. G. Busetto, E. Numminen, J. Corander, M. Foll, and C. Dessimoz. Approximate Bayesian Computation, *PLOS Computational Biology.* vol. 9. no. 1. pp. 1–10. 2013.